Eur. Phys. J. D **16**, 285–288 (2001)

THE EUROPEAN PHYSICAL JOURNAL D

EDP Sciences

Assembling of hydrogenated aluminum clusters

F. Duque[1], L.M. Molina[2], M.J. López[2], A. Mañanes[1], and J.A. Alonso[2,a]

[1] Departamento de Física Moderna, Facultad de Ciencias, Universidad de Cantabria, 39005 Santander, Spain
[2] Departamento de Física Teórica, Facultad de Ciencias, Universidad de Valladolid, 47011 Valladolid, Spain

Received 21 November 2000

Abstract. The electronic and atomic structure of $Al_{13}H$ has been studied using Density Functional Theory. $Al_{13}H$ has closed electronic shells. This makes the cluster very stable and suggests that it could be a candidate to form cluster assembled solids. The interaction between two $Al_{13}H$ clusters was analyzed and we found that the two units preserve their identities in the dimer. A cubic–like solid phase assembled from $Al_{13}H$ units was then modeled. In that solid the clusters retain much of their identity. Molecular dynamics runs show that the structure of the assembled solid is stable at least up to 150 K. A favorable relative orientation of the clusters with respect to their neighbors is critical for the stability of that solid.

PACS. 36.40.Cg Electronic and magnetic properties of clusters – 36.40.Mr Spectroscopy and geometrical structure of clusters – 61.46.+w Nanoscale materials: clusters, nanoparticles, nanotubes, and nanocrystals

The high stability of the $Al_{13}H$ cluster indicates that it could be a promising candidate for the synthesis of new cluster assembled materials [1]. The neutral cluster has a HOMO–LUMO gap of 1.4 ± 0.2 eV, measured by photoelectron spectroscopy (PES) of the $Al_{13}H^-$ anion [1]. The experimental observations are consistent with the predictions of the jellium model for aggregates of s–p elements [2]; in this model the 40 valence electrons of $Al_{13}H$ give a structure of closed electronic shells. PES experiments [3–5] and *ab initio* calculations [6] confirm the validity of the jellium model predictions for pure aluminum clusters.

In the present work we use the Density Functional Theory (DFT) [7] to study the electronic and atomic structure of $Al_{13}H$, investigating the equilibrium location of the hydrogen atom. Then, the interaction between two $Al_{13}H$ clusters is studied as a function of their distance and relative orientation. Finally an assembled cluster solid is modeled as a cubic lattice built from $Al_{13}H$ units and its stability is tested by molecular dynamics simulations.

We use DFT, with the local density approximation (LDA) for exchange and correlation [8], to study first the free Al_{13} and $Al_{13}H$ clusters . The Kohn–Sham (KS) equations [7] are solved for the valence electrons using the ADF code [9], treating the Ne–core of each Al atom as frozen. The basis set is formed by s, p, and d Slater–type atomic orbitals. For each Al atom, the basis contains three s, nine p and five d orbitals, and for H, three s and three p orbitals. The basis set is non–orthogonal. The calculation is a spin restricted, nonpolarized one. However, to obtain the correct binding energies, a spin polarized calculation is performed for the free H and Al atoms. No symmetry restrictions are imposed to the geometry of the clusters, neither to their electronic states.

We confirm that the equilibrium structure of Al_{13} is a distorted icosahedron with one central atom, a geometry found in previous *ab initio* calculations [10]. The Al–Al distances are given in Table 1. The anionic cluster Al_{13}^-, with 40 valence electrons, has a more regular icosahedral structure, with a slight contraction with respect to the neutral. In contrast, a more distorted icosahedron is obtained for the cation Al_{13}^+, with a small expansion with respect to the neutral. The calculated binding energy of Al_{13}, measured with respect to the separated atoms is given in Table 2. The binding energy is larger than the value of 35.97 eV obtained by local spin–density calculations for the perfect icosahedral structure [11]. When a spin–polarized calculation is performed for the open shell Al_{13}, a very small increase in binding energy is obtained with respect to the non-polarized result (0.05 eV), without noticeable relaxation of the geometry. This indicates that the Jahn–Teller distortions allowed for in our calculation have a much larger effect than those due to spin polarization. The HOMO–LUMO gap of the closed–shell Al_{13}^- cluster, calculated from the corresponding orbital energies, is $\Delta\epsilon = 1.81$ eV.

Several locations for the H atom bound to Al_{13} have been tried, following the suggestions of previous work [12]: top, bridge and hollow sites, and also positions inside the cage. In the top site, the atom is placed outside the Al_{13} cage, in the radial direction passing through one of the surface atoms. The bridge position corresponds to the atom above the middle of the edge connecting two neighboring Al surface atoms. In the hollow position the atom sits

[a] e-mail: jaalonso@fta.uva.es

Table 1. Bond lengths (in atomic units) for the equilibrium geometries. Distances from the central Al to the outer Al atoms are indicated by d; D are distances between neighbor Al atoms on the surface of the cluster. For the hydrogenated aggregates, dH is the distance from H to the central Al atom, and DH are H–Al nearest-neighbor distances for Al at the surface. Subscripts m and M indicate minimum and maximum values.

	d_m	d_M	D_m	D_M	$D\mathrm{H}_m$	$D\mathrm{H}_M$	dH
Al_{13}^+	5.04	5.20	5.10	6.66			
Al_{13}	5.02	5.10	5.20	5.59			
Al_{13}^-	5.04	5.05	5.26	5.33			
$Al_{13}H^+$	5.00	5.10	5.20	5.51	3.65	3.70	5.73
$Al_{13}H$	5.00	5.08	5.20	5.54	3.67	3.67	5.68
$Al_{13}H^-$	5.01	5.12	5.25	5.69	3.59	3.60	5.40

above the centre of one of the triangular faces. In each case the equilibrium structure was obtained by first moving radially the H atom, with the Al cage frozen, till a minimum of the energy is found, and at that stage a complete relaxation of the cluster was performed. The lowest energy equilibrium configuration was found for the hollow site, with the H atom at equal distances of 3.67 a.u. from the three Al atoms of the triangular face. Other relevant distances are given in Table 1. The H binding energy is 3.36 eV. The bridge and top configurations are only saddle points. A very small barrier of 0.08 eV separates hollow sites in two adjacent faces, suggesting a high mobility of the H atom over the surface at room temperature. The calculated binding energy of an isolated H_2 molecule by the present method, using the spin–polarized result for the H atom, is 4.95 eV, to be compared with the experimental value 4.75 eV. This means that there is a net energy gain of 1.77 eV when the H_2 molecule dissociates and each of the two H atoms binds to a different Al_{13} cluster. We have also investigated the possibility of placing the H atom inside the Al_{13} cage, but it was no possible to find a stable equilibrium position. The geometries of the charged clusters have been calculated starting from the equilibrium configuration of the neutrals. Data for the bond lengths are given in Table 1. In $Al_{13}H^-$, the H atom is closer to the cluster surface than in the neutral, and closer to the central Al atom as well, in spite of the small expansion of the Al_{13} cluster. For $Al_{13}H^+$, the H atom is slightly more distant from the cluster surface.

The HOMO–LUMO gap of $Al_{13}H$, estimated from the corresponding orbital energies, is $\Delta\epsilon = 1.77$ eV. This can also be obtained as the energy difference between the highest occupied molecular orbital and the next occupied orbital of the anion $Al_{13}H^-$, that provides a more convenient estimate because only occupied orbitals are involved. The corresponding value, $\Delta\epsilon = 1.63$ eV, is within the error limits of the experimental result, 1.4 ± 0.2 eV [1]. The adiabatic ionization potential of $Al_{13}H$ is $I = 7.05$ eV, in good agreement with other DFT calculation [12]. The large value of I reflects the high stability of the aggregate. The calculated adiabatic electron affinity is $A = 1.76$ eV.

Table 2. Energies of the highest occupied orbital ϵ_{HOMO}, HOMO–LUMO gap $\Delta\epsilon$, and cluster binding energy BE with respect to the separated atoms, in eV.

	ϵ_{HOMO}	$\Delta\epsilon$	BE
Al_{13}^+	−7.43	0.73	
Al_{13}	−3.95		39.22
Al_{13}^-	−0.87	1.81	
$Al_{13}H$	−4.11	1.77	42.58
$(Al_{13}H)_2$	−3.14	0.70	88.18

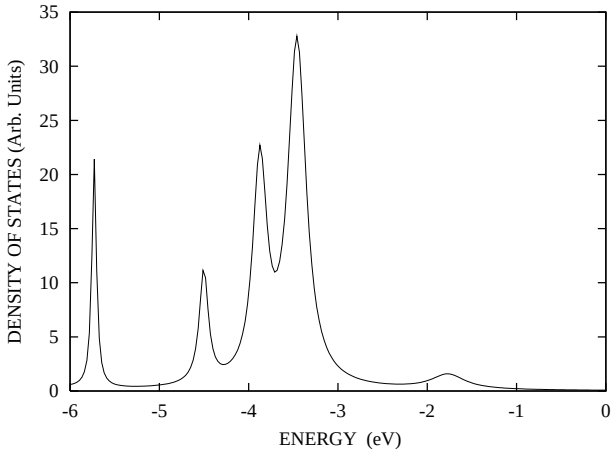

Fig. 1. Calculated electronic density of states (DOS) for $Al_{13}H^-$ with the H atom in the hollow position.

Comparison between the calculated electronic density of states (DOS) of $Al_{13}H^-$ and the measured PES spectrum [1] allows to discuss the location of the H atom.

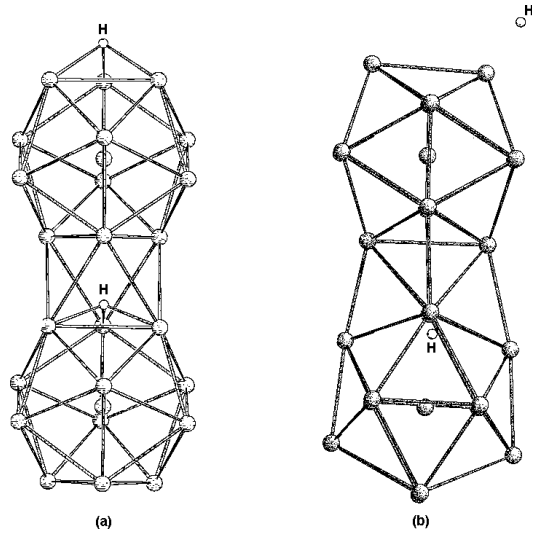

Fig. 2. Two isomeric geometries of $(Al_{13}H)_2$. The ground state is isomer (b) and isomer (a) is 1.28 eV above in energy.

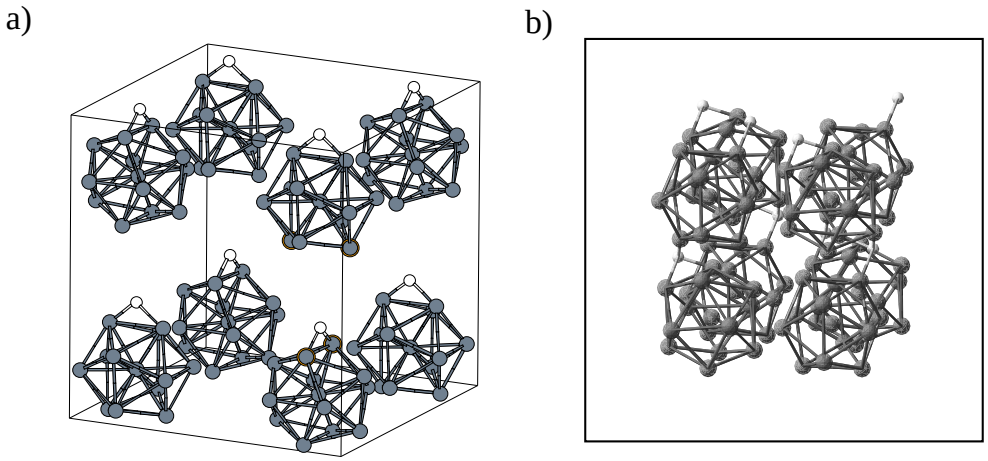

Fig. 3. Unit cell of the assembled solid for a large value of the lattice constant (a), and snapshot of the structure near the equilibrium volume for a dynamical simulation at 150 K (b).

To obtain the DOS we start with the KS single–particle states. The eigenvalue of the highest–occupied KS orbital, ϵ_{HOMO}, gives the ionization potential, I, (that is $I = -\epsilon_{HOMO}$) for the exact exchange–correlation functional [13,14]. However, for the usual approximate continuum functionals that relation is not fulfilled. Instead, a generalized Koopman's theorem is obtained for I [15]:

$$I = -\epsilon_{HOMO} + v_{xc}(\infty), \qquad (1)$$

where $v_{xc}(\infty)$ is the asymptotic value of the exchange–correlation potential. This equation can be used to calculate $v_{xc}(\infty)$ as the actual energy shift between I (obtained as the difference between the energies of the ionized and neutral species) and $-\epsilon_{HOMO}$. The value $v_{xc}(\infty)$ is then applied as a rigid shift to all the KS energies to improve the absolute energy scale of the electronic spectrum [3,15]. For the anion $Al_{13}H^-$ with the H atom at the hollow site, the value $v_{xc}(\infty) = 2.36$ eV has been used to calculate the DOS given in Fig. 1, where each KS energy has been broadened by a normalized Lorentzian of width comparable to the experimental resolution [1,4]. The structure of the spectrum is in good agreement with experiment, in particular the small feature at -1.8 eV and the distance between this and the next large feature, that can be identified with the HOMO–LUMO gap of the neutral. In contrast, when the H is at the top location, the DOS shows an energy gap too small compared to experiment.

Next we have studied the dimer $(Al_{13}H)_2$. The cluster $Al_{13}H$ has a static dipole moment of 0.28 Debye, in the direction of the H atom. We first consider two clusters with a fixed relative orientation, chosen so as to maximize the dipole–dipole interaction. A "head to tail" geometry was constructed in which the clusters are face to face and one of them is rotated by $\pi/3$ about the axis joining the two centers, with one H atom between the two clusters and the other on the outer opposite face. The energy was calculated for several intercluster distances without any relaxation of the cluster geometries, and a minimum was obtained for a distance $R_m = 11.81$ a.u. between the cluster centers. For the geometry at R_m a steepest descent relaxation of the structure was then performed, and the resulting equilibrium geometry is given in Fig. 2(a), which shows that the two clusters preserve their structures in the dimer. The relaxation had a very small effect on the structure of the dimer and the calculated binding energy with respect to the two separated clusters, is 1.78 eV. The intracluster interatomic distances experience small changes with respect to those in the separated clusters. The smallest intercluster Al–Al distances have values between 5.59 a.u. and 5.72 a.u., and comparison with those in Table 1 indicates that they are only a little larger than the intracluster distances. The structure has an approximate C_{3v} symmetry. Nevertheless, there is a different isomer, in fact more stable than the one just discussed. Its structure is shown in Fig. 2(b), and the relevant energies are given in Table 2. The main structural difference is that the clusters have contact Al–Al edges perpendicular to each other, that is, one cluster is rotated 90 degrees with respect to the other. The H atom of the bottom cluster adopts a bridge position inside the cluster. The other H atom is located on a top position in the upper cluster. The binding energy of the dimer with respect to two $Al_{13}H$ units is 3.03 eV, and the gain of 1.25 eV is due to the favorable orientation of the units. A similar structure was found as the ground state for the $(Al_{13})_2$ dimer in pair potential calculations [16]. As a consequence of the cluster–cluster interaction, near–degeneracies of electronic levels split and shells broaden. Consequently the HOMO–LUMO gap is reduced to 0.71 eV. Of course, there is some freedom for the initial locations of the H atoms, that could lead to different final positions for those atoms. We have not investigated this point in detail because, as shown below, the H atoms easily find their way to their optimal location in the simulations of the assembled solid.

We have modeled the assembling of $Al_{13}H$ clusters with a Car-Parrinello type code [17] that uses a supercell geometry, a basis set of plane waves and nonlocal norm–conserving pseudopotentials. The plane wave energy cutoff was set at 25 Ry. The forces on the atoms were calculated by means of the Hellmann-Feynman theorem, and the molecular dynamics simulations at constant temperature were performed with a Nosé–Hoover thermostat.

The optimal relative cluster–cluster orientation in the ground state of the dimer suggests that the structure to

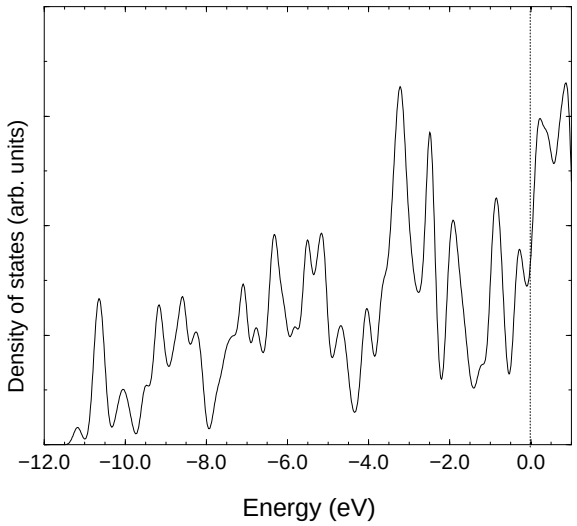

Fig. 4. Electronic DOS of the assembled cluster solid near the end of a molecular dynamics simulation at 150 K.

be tried for the assembled solid should be one in which each cluster is alternated 90 degrees with respect to all its nearest clusters, in order to have the closest edges between cluster neighbors perpendicular to each other. The number of cluster neighbors is then 6 and this leads to a structure of a simple cubic lattice with 8 clusters per unit cell [18]. For simplicity the H atom is placed in a bridge position at the beginning of the simulation, although this is not crucial. In a first step the energy of the assembled solid was calculated as a function of the lattice constant, maintaining the component clusters frozen. Figure 3(a) shows the structure of that solid for a lattice constant such that the clusters are well separated. Two energy minima were obtained. The outer minimum, that corresponds to a lattice constant of 32 a.u., has a binding energy of 0.35 eV per cluster (with respect to the separated clusters). In this configuration the Al atoms of neighbor clusters are well separated. A second, deeper minimum is found, with a large binding energy of 15 eV per cluster and a smaller lattice constant of 24.2 a.u. In this case the Al–Al intercluster distances become comparable to the intracluster distances. Although a value of the binding energy of 15 eV is large, that number is still small with respect to the internal binding energy of the clusters with respect to the separated atoms, which is 42.58 eV as given in Table 2. The assembled solid has a gap at the Fermi energy for the volume corresponding to the small outer minimum but no gap occurs for the main deep minimum.

At that point we fully relaxed the atomic coordinates. For that purpose we performed constant temperature dynamical simulation runs at 150 K, for a cell with a lattice parameter of 24.0 a.u. The time step was 5 fs and the total simulation time was about 3 ps. The results show that at that temperature the assembled solid is stable against deformations that could induce a transition to another structure. Figure 3(b) shows a snapshot near the end of the trajectory in one of the simulations. Although the Al_{13} units are connected and a little bit distorted, they retain the icosahedral structure along the trajectory. The main effect of the temperature is to allow the H atoms to migrate from their initial positions to more favorable interstitial places within the cubic arrangement of clusters. The energy gain due to this migration is about 0.7 eV per H atom. In summary, the assembling of the $Al_{13}H$ clusters leads to a cluster solid that appears to be stable at least up to 150 K. The density of states, given in Fig. 4 shows that the assembled solid has metallic character. We have also performed simulations for a more compact solid. An fcc-type lattice of $Al_{13}H$ clusters was constructed and the atomic positions were relaxed for various values of the lattice constant. In this case the interaction between the clusters is much larger and they lose completely their individual character. The structure obtained cannot be considered any more as a solid of clusters. In the fcc lattice each icosahedral cluster has twelve neighbor clusters and the favorable orientational requirements are not met. The conclusion is that the relative orientation of the clusters, that controls the degree of packing in the lattice, plays an important role, in addition to other obvious requirements like a high intrinsic stability of the individual clusters. That stability arises from a combination of electronic (large HOMO–LUMO gap) and structural factors.

Work supported by DGESIC of Spain (Grants PB98-0190 and PB98-0345). Computational resources of CESCA and CEPBA, coordinated by C^4, are acknowledged.

References

1. S. Burkart, N. Blessing, B. Klipp, J. Müller, G. Ganteför, G. Seifert, Chem. Phys. Lett. **301**, 546 (1999).
2. W. de Heer, Rev. Mod. Phys. **65**, 611 (1993).
3. J. Akola, M. Manninen, H. Häkkinen, U. Landman, X. Li, L.S. Wang, Phys. Rev. B **60**, 11297 (1999).
4. X. Li, H. Wu, X.B. Wang, L.S. Wang, Phys. Rev. Lett. **81**, 1909 (1998).
5. G. Ganteför, W. Eberhardt, Chem. Phys. Lett. **217**, 600 (1994); C.Y. Cha, G. Ganteför, W. Eberhardt, J. Chem. Phys. **100**, 995 (1994).
6. F. Duque, A. Mañanes, Eur. Phys. J. D **9**, 223 (1999).
7. W. Kohn, *Density Functional Theory*, edited by E.K.U. Gross, R.M. Dreizler (Plenum Press, New York, 1995).
8. S.H. Vosko, L. Wilk, M. Nusair, Can. J. Phys. **58**, 1200 (1980).
9. G. te Velde, E.J. Baerends, J. Comput. Chem. **99**, 84 (1992); P.M. Boerriger, G. te Velde, E.J. Baerends, Int. J. Quantum Chem. **33**, 87 (1988).
10. J.E. Fowler, J.M. Ugalde, Phys. Rev. A **58**, 383 (1998).
11. X.G. Gong, V. Kumar, Phys. Rev. Lett. **70**, 2078 (1993).
12. S.N. Khanna, P. Jena, Chem. Phys. Lett. **218**, 383 (1994).
13. J.P. Perdew, M. Levy, Phys. Rev. B **56**, 16021 (1997).
14. C.O. Almbladh, U. von Barth, Phys. Rev. B **31**, 3231 (1985).
15. D.J. Tozer, N.C. Handy, J. Chem. Phys. **109**, 10180 (1998).
16. D.Y. Sun, X.G. Gong, Phys. Rev. B **54**, 17051 (1996).
17. M. Bokstedte, A. Kley, J. Neugebauer, M. Scheffler, Comput. Phys. Commun. **107**, 197 (1997).
18. X.G. Gong, Phys. Rev. B **56**, 1091 (1997).